

HIDDEN ANCESTOR GRAPHS WITH ASSORTATIVE VERTEX ATTRIBUTES

R. W. R. DARLING

National Security Agency, Fort George G. Meade, MD 20755-6844, USA

ABSTRACT. The hidden ancestor graph is a new stochastic model for a vertex-labelled multi-graph G in which the observable vertices are the leaves L of a random rooted tree T , whose edges and non-leaf nodes are hidden. The likelihood of an edge in G between two vertices in L depends on the height of their lowest common ancestor in T . The label of a vertex $v \in L$ depends on a randomized label inheritance mechanism within T such that vertices with the same parent often have the same label. High label assortativity, high average local clustering, heavy tailed vertex degree distribution, and sparsity, can all coexist in this model. The agreement edges (end point labels agree) and the conflict edges (end point labels differ) constitute complementary subgraphs, useful for testing anomaly correction algorithms. Instances with a hundred million edges can easily be built on a workstation in minutes.

Keywords: complex network, random graph, stochastic model, random walk

MSC class: Primary: 05C80; Secondary: 90C35

E-mail address: `rwdarli@nsa.gov`.

Date: March 1, 2025.

CONTENTS

1. Attributed graph models	4
1.1. Desired properties	4
1.2. Properties of other models	4
1.3. Conflict graph versus agreement graph	5
1.4. Hidden ancestor graph: high level view	5
1.5. Concrete examples where hidden ancestor graph models may apply	8
2. Constructing the latent tree and its labels	9
2.1. Tree notation	9
2.2. Node label generation in the latent tree	9
3. A minimal parametrization for a hidden ancestor graph	10
3.1. Three probability distributions	10
4. Hidden ancestor graph: edge construction	11
4.1. Transition probabilities for a random walk on the tree	11
4.2. Edge creation using pairs of random walks	12
4.3. Construction of the edges via matching	13
4.4. How the matching construction compares with random walk pairs	13
5. The depth one hidden ancestor graph in full detail	14
5.1. Construction	15
5.2. Statistics of the depth one case	15
6. Decoupling times for pairs of random walks	16
6.1. Assumptions about the latent tree	16
6.2. Hitting probabilities of random walk on the tree	16
6.3. Decoupling estimates	17
6.4. Agreement edge and conflict edge estimates	19
7. Mean clustering in the agreement graph	21
7.1. Average local clustering coefficient	21
7.2. Sibling subgraph	21
7.3. Mean vertex degree	22
7.4. Mean clustering coefficient heuristic	22
8. Color change parameter	23
8.1. Number of nodes in the latent tree	23
8.2. Expected number of distinct labels	23
9. Fitting a model with high clustering coefficient	23

HIDDEN ANCESTOR GRAPHS WITH ASSORTATIVE VERTEX ATTRIBUTES	3
9.1. Input data	23
9.2. A simplified fit: the cube root principle	24
9.3. Choice of depth	25
9.4. Color change rate	25
9.5. One-parameter model for height distribution	25
9.6. Exploring the height distribution	25
9.7. Summary and concrete examples	26
10. Implementation of the hidden ancestor graph	27
10.1. Hidden ancestor graph software	27
10.2. Vertex degree distribution: the log-normal option	27
10.3. Maximum likelihood for the log-normal	27
10.4. Practical steps for a hidden ancestor graph with log-normal leaf marks	28
11. Future work: label frequencies in the agreement graph	28
11.1. Label frequency fitting problem	28
11.2. Color decomposition of Galton-Watson trees	29
11.3. A one-parameter model of component sizes in the agreement graph	30
Acknowledgments	31
Appendix A. Repeated weighted sampling	31
Appendix B. Constrained MLE of log-normal parameters	33
References	34

1. ATTRIBUTED GRAPH MODELS

1.1. Desired properties. The motivation for the class of models presented here is to compare and validate anomaly-correction algorithms on sparse vertex-labelled graphs with tens of millions of vertices and hundreds of millions of edges. Correcting anomalous labels is usually necessary in any kind of combinatorial data fusion [5]. Algorithm testing is more efficient when applied to models which are tens or hundreds of times smaller than, but with local properties similar to, the original; see [4].

Algorithms will be applied to vertex-labelled graphs arising in geospatial information systems, communication networks, and social networks, among other contexts. Such graphs often have the following properties:

- a. **Sparsity:** most vertices have low degree.
- b. **Heavy tailed** vertex degree distribution, such as the log normal: a few vertices have very high degree.
- c. High global **clustering** coefficient: if $v' \sim v$ and $v'' \sim v$, then there is a better than random chance that $v' \sim v''$, where the notation $v' \sim v$ denotes adjacency of v' and v .
- d. **Assortative** labels: if $v \sim v'$, there is a good chance that v and v' have the same label.

There are two other properties we would like our models to have:

- e. **Parsimony:** Half a dozen parameters should suffice to control graph characteristics mentioned above.
- f. **Scalability:** Graphs from 1% scale to 100% scale should be fast and easy to construct, given sufficient memory.

1.2. Properties of other models. There are a variety of other generative models, which offer some but not all of the properties a. to f.

- The **stochastic block model** [16] initially partitions vertices into color classes, and then prescribes a connection rate between each pair of vertices that depends only on the color class to which each belongs. Sparse models with a moderate number of color classes do not permit high clustering rates.
- **Preferential attachment graphs**, as described in Frieze & Karonski [7, Chapter 17], allow construction of graphs with heavy-tailed degree distributions, and can be modified to allow for high clustering [1], but lack a natural way to assign assortative labels to vertices.
- Sathanur, Choudhury, Joslyn, and Purohit [14] present a **property graph model** which allows a specific relationship between vertex labels and network structure to be realized in a graph. Clustering is not specifically enabled.
- The **random overlapping communities** model of Petti & Vempala [12] allows adjustment of the clustering coefficient as well as the degree distribution, but does not offer a structurally related system of vertex labelling.
- Seshadri, Kolda, and Pinar [15] have defined a **block two-level Erdős-Rényi model** (BTER) which is able to synthesize graphs with a given degree distribution, as well as a given dependence of clustering coefficient on degree. It is possible to build a separate

BTER model for each color class, and then add extra edges connecting vertices in different color classes. This achieves the goals above, except that the inputs would have to be given in functional form to achieve parsimony.

1.3. Conflict graph versus agreement graph. Let $G := (V, E, w)$ be an edge-weighted, undirected graph, with weight function $w : E \rightarrow (0, \infty)$. G need not be connected, but we assume there are no isolated vertices. Let \mathcal{A} be a finite alphabet, and let

$$\chi : V \rightarrow \mathcal{A}$$

be a **vertex labelling** function. Partition the edge set as $E = E_a \cup E_c$, where

$$E_a := \{\{v, v'\} \in E : \chi(v) = \chi(v')\}; \quad E_c := \{\{v, v'\} \in E : \chi(v) \neq \chi(v')\};$$

Call E_a the **agreement edges** and E_c the **conflict edges**, respectively. The edge-induced subgraphs $G_a := (V_a, E_a, w)$ and $G_c := (V_c, E_c, w)$ are called the agreement graph and conflict graph, respectively. The term *edge-induced* means that V_a is precisely the subset of V with at least one incident agreement edge, and so on. V_a and V_c need not be disjoint, because a vertex may be incident to edges of both types; see Figure 4. For each of these subgraphs, we have restricted the weight function to the selected edges.

We shall loosely call the vertex labelling function **assortative**¹ when most of the edges of the graph are agreement edges. The conflict edges are viewed as an anomalous minority. If there were no conflict edges, then the graph would decompose into monochromatic connected components.

1.4. Hidden ancestor graph: high level view. This section supplies the reader with a high level view of the hidden ancestor graph construction, shorn of mathematical detail.

1.4.1. The latent rooted tree. Begin by constructing a rooted tree where all leaf nodes are at the same depth; this condition could be relaxed, but it makes computation easier. Galton-Watson processes (where each non-leaf node has at least one offspring) provide a suitably diverse set of random trees; here we refer to the tree representing the entire genealogy of a branching process, discussed in standard texts such as Grimmett and Stirzaker [8], and examined further in Lyons and Peres [9]. The law of this random rooted tree is specified by an offspring distribution on the integers, and a depth.

The root is assigned a color label. There is a stochastic mechanism whereby every remaining node either adopts the color of its parent (typical), or else creates a novel² color (less common). See Figure 1. None of the edges or non-leaf vertices of this tree will appear in the hidden ancestor graph itself.

1.4.2. Marking leaf vertices, and deciding wildness. Select a probability distribution on the positive reals, from which we generate a random variate independently for each leaf node, and attach the variate to that node. See Figure 2. This **leaf mark** will represent the mean number of attempts to connect an edge of the hidden ancestor graph to that leaf.

Independent Bernoulli trials, with a fixed success rate, are used to determine whether a leaf vertex is **wild** (rare) or **tame** (typical). The Bernoulli trial for determining wildness at a

¹Not to be confused with assortativity in the sense of degree correlation between adjacent vertices.

²Novel means not found among any node at the same or lesser depth.

FIGURE 1. **Latent tree with vertex labels:** The root vertex is shown at the center. One of its children inherits the root's color, and the other starts a novel color. Four generations are shown. In most cases, leaf nodes with a common parent all have the same color. The reds at top right, bottom right, and bottom left, are actually different colors, as one can see from their ancestry.

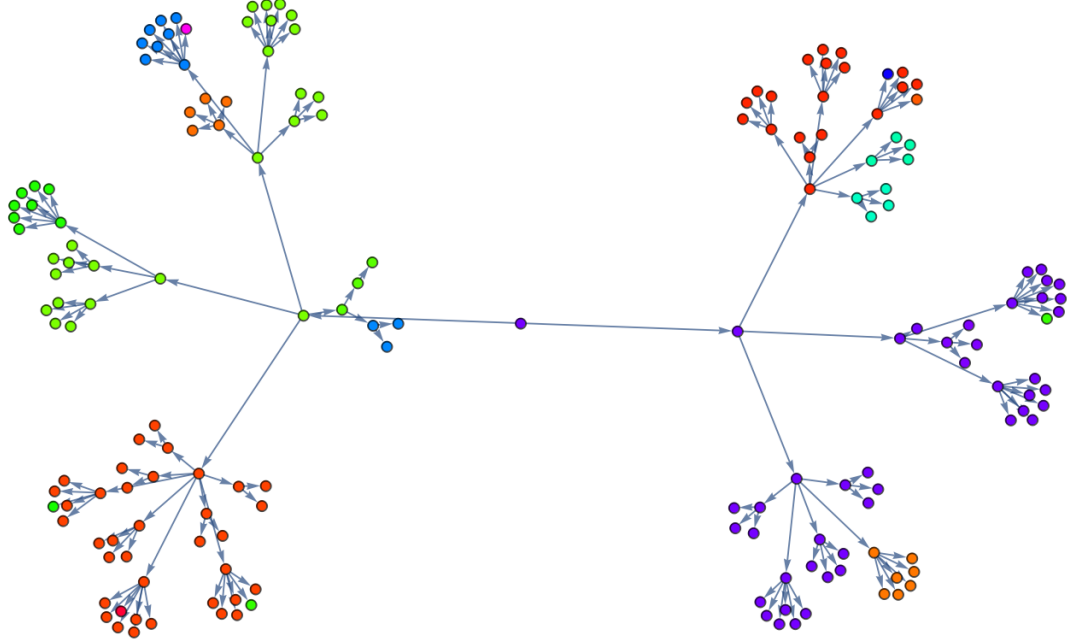
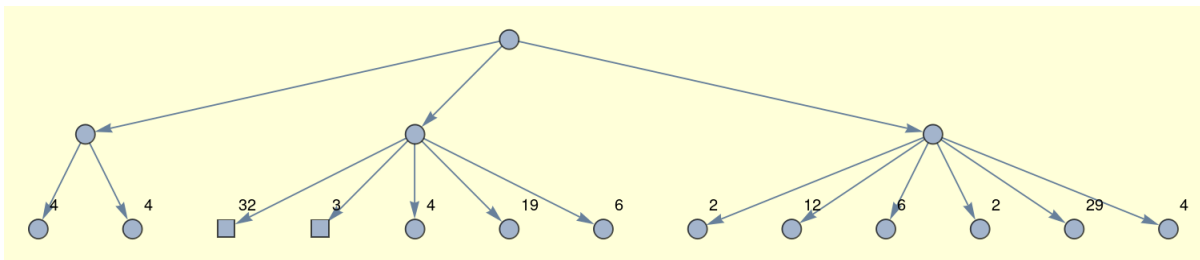


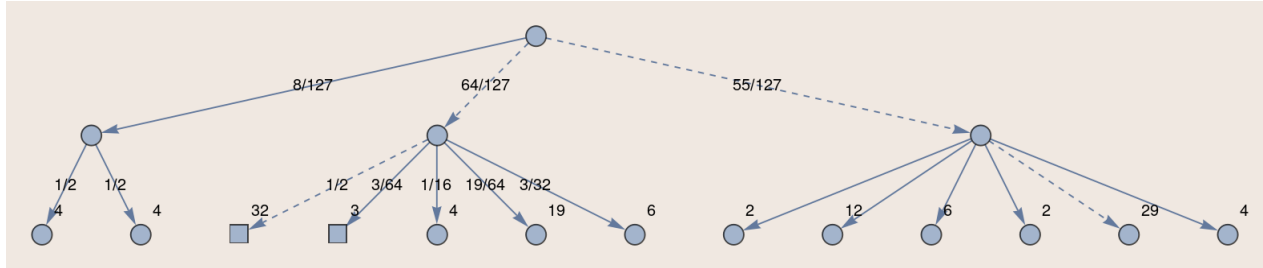
FIGURE 2. **Frequency marks on leaves of latent tree:** Attach to each leaf vertex of the latent tree a random variate sampled independently from a specific distribution on $(0, \infty)$. In this example, ceilings of log normal random variates are shown. Wild vertices are marked \square , tame vertices by \circ .



leaf node need not be independent of the mark at that node. Introducing positive dependence can be a tool for influencing the structure of the conflict graph.

1.4.3. *Directed random walks on the latent tree.* There is a natural random walk on the nodes of the latent tree, in which the leaf nodes are absorbing states. If the current state is a non-leaf node, the next state must be one of the children of that node. The probability of choosing a particular child is proportional to its mark if that child is a leaf, or to the sum of frequency marks of leaf nodes descended from that child otherwise. See Figure 3, and the example in

FIGURE 3. **Transition probabilities for directed random walks:** *If the current state is a non-leaf node, the next state must be one of the children of that node. Transition rates are proportional to the sum of frequency marks of leaf descendants. For example, transitions from the root shown to the middle child occur with probability $64/127$. Transitions from that child to its leftmost wild offspring occur at rate $32/64 = 1/2$. Dashed arrows show two random walks from the root, terminating at leaves marked 32 and 29, respectively. Since the former is wild, an edge in the hidden ancestor graph will be created, regardless of the color labels of the leaves.*



the caption. For any given starting node v , the terminal state of a random walk started at v is a Multinomial draw from the leaf nodes descended from v , weighted by their leaf marks, as we shall establish in Lemma 6.1.

1.4.4. Edge generation based on pairs of random walks. The vertex set of the hidden ancestor graph is the set of leaf nodes of the latent tree. The mechanism for generating an edge of the hidden ancestor graph goes as follows. It depends on a probability distribution on depths $\{0, 1, \dots, D - 1\}$, where D denotes the depth of a leaf node of the latent tree.

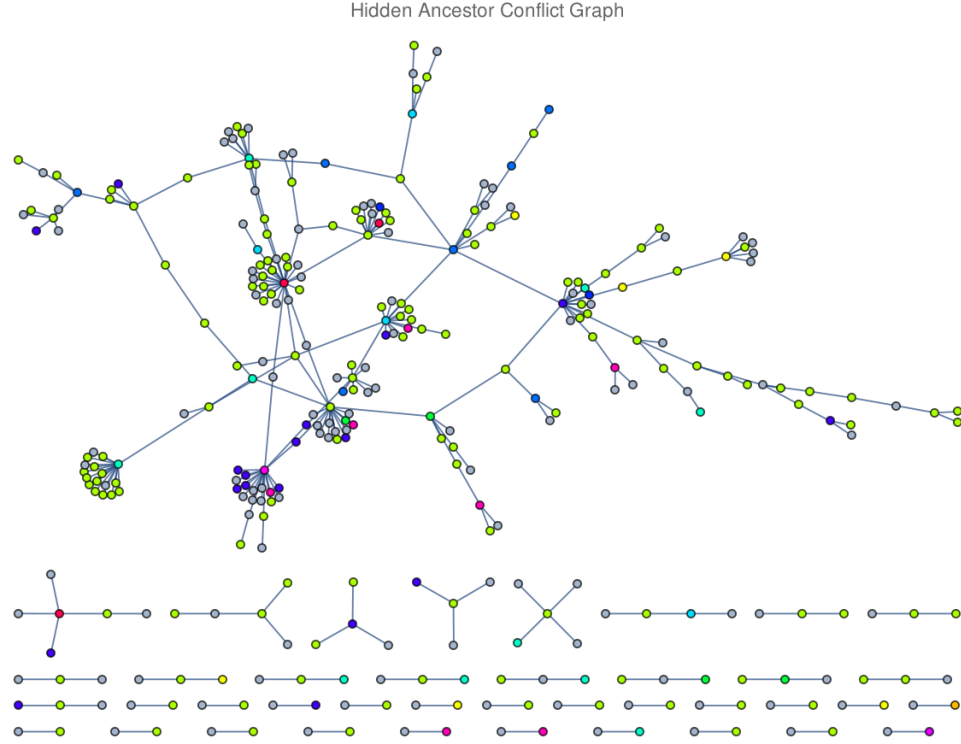
- (1) Generate a random depth d in $\{0, 1, \dots, D - 1\}$.
- (2) Sample one of the nodes at depth d , with probabilities proportional to node weight. Call this the **start node**.
- (3) Start two independent random walks at the start node, as illustrated in Figure 3.
- (4) Let the terminal states of these two walks be leaf nodes v, v' , respectively. If $v \neq v'$, then an edge $\{v, v'\}$ is inserted in the hidden ancestor graph provided either
 - v and v' have the same color tag, or
 - at least one of v and v' is a wild vertex.

The expected number of edge generation attempts is half the sum of all the leaf marks. We expect a significant proportion of attempts to fail, either because the two random walks have the same end point, or else because both end points are tame and yet their color labels differ. The same edge may occur m times, in which case we assign weight m to this edge.

A miniature example of the conflict graph of a hidden ancestor graph is shown in Figure 4.

1.4.5. Summary of the choices for building a hidden ancestor graph. The modeller must choose:

FIGURE 4. **Conflict Graph:** *hidden ancestor graph edges whose end points have different labels.*



- (1) The *offspring distribution* and *depth* of the latent tree. These choices determine the expected number of leaf nodes, which in turn constitute the vertex set of the hidden ancestor graph.
- (2) The *color inheritance mechanism* for nodes in the tree. Typically this is depth-dependent, and affects the number of distinct labels seen in the hidden ancestor graph.
- (3) The *probability distribution for leaf marks*, which governs the vertex degree distribution of the hidden ancestor graph.
- (4) The *wildness rate*, and possible correlation of wildness with leaf mark, which affect the relative size of the conflict graph.
- (5) The *depth distribution* for random walk start points, which affects the clustering coefficient.

This seems like a lot of moving parts. However each of them can be made simple enough that predictive nonlinear formulas can be written down for observable graph properties in terms of half a dozen parameters, as we shall do in Sections 6, 7, and 8. In Section 9 we solve for these parameters so as to build a hidden ancestor graph with desired properties.

1.5. Concrete examples where hidden ancestor graph models may apply. Here are several sorts of large labelled networks where a latent tree can plausibly explain some of the structure. In real examples, wild and tame status are inferred from graph structure, rather than provided *a priori*.

1.5.1. *Genotypes versus phenotypes.* Living organisms are leaves of the phylogenetic tree, whose hidden nodes are ancestors from whom genotype is inherited. Label these nodes by a specific set of genetic mutations. Take a set of phenotypes, i.e. observable characteristics of organisms. Insert an edge between two leaves if they share sufficiently many phenotypes. A conflict edge means a pair of organisms with shared phenotypes, but different genetic mutations. A wild vertex means an organism whose observable characteristics are similar to those with different genetic mutations, which implies that those characteristics are not indicative of genotypes.

1.5.2. *Merchandise categorization for online retailing.* Items offered for sale in an online marketplace are leaves of a tree, whose hidden nodes are the suppliers and industries which created them. Labels are consumer categories, such as *DIY hardware, men's apparel*. Collect online transactions over a suitable time period, and connect two items by an edge if they appear in the same shopping basket for a sufficiently large number of baskets. A conflict edge means a pair of items appearing in the same shopping baskets, but with different product categories. A wild vertex means an item which perhaps defies categorization, because it often appears in the same basket as seemingly unrelated items; perhaps it requires a different marketing strategy.

1.5.3. *Distributed communication networks.* The points at which users gain access to a large communications network are typically leaf nodes of a tree-structured network of servers and routers. Label these access points by spatial zones. Insert an edge between two access points if at least one user uses both of them within a short time period. Most edges connect access points in the same spatial zone. Some access points may serve users in multiple spatial zones. These will be the wild vertices.

2. CONSTRUCTING THE LATENT TREE AND ITS LABELS

2.1. **Tree notation.** We shall need:

- (1) A **rooted tree** (V, T) with root v_o , and depth D . Every $v \in V \setminus \{v_o\}$ has a unique **parent**, denoted $\pi(v)$, which is the next vertex on the unique path towards the root. Denote by V_d the set of vertices $v \in V$ whose d -ancestor $\pi^d(v)$ is v_o . Elements of V_d are at **depth** d from the root, and also at **height** $D - d$ above the leaves.
- (2) Parameters $\rho_1, \rho_2, \dots, \rho_D \in [0, 1]$ for Bernoulli random variables determining **label inheritance** in the rooted tree. These in turn will determine the probability law of labels assigned to the leaves L , as we shall now describe.

2.2. **Node label generation in the latent tree.** Let $\{Z_v, v \in V \setminus \{v_o\}\}$ be independent Bernoulli random variables, whose mean depends on the depth of vertex v . Indeed, for depths $d = 1, 2, \dots, D$,

$$\mathbf{E}[Z_v] = \rho_d, \quad \forall v \in V_d.$$

The labelling rule is:

- The root node v_o acquires label 0.
- If $Z_v = 0$, then node v acquires the same label as its parent $\pi(v)$.
- If $Z_v = 1$, and $\{0, 1, \dots, k-1\}$ is the set of previously assigned labels, then node v is assigned label k .

Assignment of labels is shown by the colors in Figure 1, and symbolized by a map

$$(1) \quad \chi : V \rightarrow \mathcal{A} := \{0, 1, \dots, K - 1\}$$

where $K := |\mathcal{A}| = 1 + \sum_{1 \leq t < |V|} Z_t$ is a random variable denoting the number of distinct labels. We shall use the terms *label* and *color* interchangeably. In our simulations, we shall set $\rho_1 = 1$ (so each child of the root starts a new color), and $\rho_D = 0$ (so that leaf vertices with a common parent have the same color).

Definition 2.1. *The canonical Poisson labelled tree, with parameters $(\mu, D, \theta) \in \mathbf{Z}_+ \times \mathbf{Z}_+ \times (0, \infty)$ is the special case of the above construction, where (V, T) is a Galton-Watson tree of depth D , with a $1 + \text{Poisson}(\mu - 1)$ offspring distribution³ and the parameters (ρ_d) take the form $\rho_D = 0$, and*

$$(2) \quad \rho_d := \frac{\theta}{\theta - 1 + \mu^0 + \dots + \mu^{d-1}} = \frac{\theta(\mu - 1)}{(\theta - 1)(\mu - 1) + \mu^d - 1}, \quad d = 1, \dots, D - 1.$$

Remark: This definition (2) is inspired by the Polya urn scheme called the Chinese Restaurant Process (CRP - see Pitman [13]). The assignment of labels to vertices may be compared to the assignment of customers to tables in the CRP. In the CRP, the probability that the n -th customer occupies a new table is $\theta/(\theta + n - 1)$; otherwise this customer sits down at the table of a previous customer, selected uniformly at random. In our tree model, on the other hand, the color is passed from parent to child in the tree. The dependencies are different, in that two vertices with the same parent are likely to have the same color, whereas two consecutive diners entering the restaurant will usually occupy different tables. To preserve symmetry among all vertices at depth d , we replace $n - 1$ (the number of customers already seated in the restaurant) by the expected number of offspring of all previous generations, and adjust the success rate of the Bernoulli trials only between generations.

In Section 10 we shall illustrate the distribution of color frequencies which results from this pattern.

3. A MINIMAL PARAMETRIZATION FOR A HIDDEN ANCESTOR GRAPH

3.1. Three probability distributions. Given the latent tree of depth D , with leaves L , three probability distributions are needed for the hidden ancestor graph itself. The random variables are all independent of any random variables used to construct the latent tree and its labels.

- (1) A probability distribution (q_1, q_2, \dots, q_D) on the integers $1, 2, \dots, D$, to be used for selecting a **random height** in the tree. The parameter q_1 plays a key role in controlling local clustering, as we shall see in Section 7.2; for the hidden ancestor graph to have a giant component, which is desirable, we need $q_D > 0$, i.e. some pairs of random walks start at the root node.
- (2) A distribution on \mathbf{R}_+ from which to sample positive real numbers $\{F_x, x \in L\}$, called **leaf marks**; marks are not the same as labels.. The mark F_x will appear later as the mean number of attempts to construct edges incident to leaf x in the hidden ancestor graph.

³I.e. $1 + \zeta$ offspring, where $\zeta \sim \text{Poisson}(\mu - 1)$. At least one child is guaranteed for every node, to ensure that all leaves occur at depth D .

(3) A joint distribution for Boolean variables $\{\eta_x, x \in L\}$ which assign each leaf vertex to either **wild** or **tame** status. Possibly η_x and F_x are statistically dependent, but the random vectors $\{(F_x, \eta_x), x \in L\}$ are mutually independent.

We now describe a minimal way to parametrize the choices spelled out in Section 1.4.5. It is tacitly assumed that agreement edges outnumber conflict edges, that most clustering occurs in the agreement graph, and that wild vertices are a minority.

Definition 3.1. *Given a depth D rooted tree (V, T) with leaves L , the **canonical hidden ancestor graph** with parameters $(q_1, \mu_f, \sigma_f^2, \omega) \in \mathbf{R}_+^4$, where $q_1, \omega \in [0, 1]$, uses the following distributions:*

- Choose height distribution (q_1, q_2, \dots, q_D) with $q_d := (1 - q_1)/(D - 1)$ for $2 \leq d \leq D$.
- Sample $\{F_x, x \in L\}$ from a distribution⁴ on $(0, \infty)$ with mean ν and variance η^2 .
- Sample $\{\eta_x, x \in L\}$ from i.i.d Bernoulli(ω).

There is a variation which uses a small **bias parameter** $\beta > 0$, such as $\beta = 0.25$, to introduce positive dependence between η_x and F_x . It uses the fact that, if $Z \sim \text{Normal}(0, 1)$, then

$$e^{\beta Z - \beta^2/2}$$

has mean 1. Say $\{Y_x, x \in L\}$ are $\text{Normal}(0, 1)$ random variables, and $\{U_x, x \in L\}$ are $\text{Uniform}(0, 1)$ random variables, all mutually independent. Take F_x to be the lognormal random variable:

$$F_x := e^{\mu_o + \sigma_o Y_x},$$

and then set $\eta_x = 1$ if

$$(3) \quad U_x < \omega e^{\beta Y_x - \beta^2/2}.$$

The effect is that large positive values of Y_x cause both an unusually large mark F_x , and an elevated wildness probability, while keeping the overall wildness rate at ω .

4. HIDDEN ANCESTOR GRAPH: EDGE CONSTRUCTION

4.1. Transition probabilities for a random walk on the tree. The random walks we shall now describe are central to the hidden ancestor graph edge construction. Random walks on Galton-Watson trees are treated in depth in Lyons and Peres [9, Chapter 17]. Our random walks are of a simpler kind, in that only transitions away from the root are allowed.

Extend the marks $\{F_x, x \in L\}$ on the leaves to marks $\{F_v, v \in V\}$ on all the nodes of the latent tree, by taking F_v to be the sum of marks in $L(v)$, the set of leaf vertices descended from v :

$$(4) \quad F_v := \sum_{x \in L(v)} F_x; \quad v \in V_d.$$

A miniature example was displayed in Figure 3. In particular, the root node has a mark:

$$F_{v_o} = \sum_{x \in L} F_x.$$

⁴Typically a heavy-tailed distribution, such as the log-normal; see the discussion in [10] and [2]. See (41) for lognormal parameters.

This leads to the definition of a **random walk** on V , whose transition probabilities are as follows.

- The leaves L are absorbing states.
- For any non-leaf vertex $v \in V$, the only possible transitions are to children of v , selected according to the conditional probabilities (given the leaf marks)

$$(5) \quad p_{v,v'} = \frac{F_{v'}}{F_v}; \quad v' \in \pi^{-1}(v),$$

which add up to one by (4).

4.2. Edge creation using pairs of random walks. Our theoretical analysis of hidden ancestor graphs uses pairs of random walks. Our software implementation uses an almost equivalent matching construction: see Section 4.3.

Denote the sum of the leaf marks by

$$(6) \quad M := \sum_{x \in L} F_x.$$

The number of attempted edge creations, conditional on the leaf marks, will have a conditional mean of $M/2$. The precise distribution need not be specified; for example, it could be $\text{Poisson}(\frac{M}{2})$, or (in the matching construction below) a sum of binomial random variables. The actual number $|E|$ of edges created will be less than this by a predictable factor, which takes account of loops, etc.

Let \mathcal{H} be a random variable taking values in $\{1, 2, \dots, D\}$, with the probability distribution $q_d := \mathbf{P}[\mathcal{H} = d]$. Here \mathcal{H} is short for *height* of the starting point above the leaves. Only one vertex has height D , namely the root. Let $\{\mathcal{H}_i\}$ be a collection of independent copies of \mathcal{H} . Our procedure for the i -th edge generation attempt will be:

- If $\mathcal{H}_i = s$, sample a non-leaf vertex v at depth $D - s$ from the root according to the distribution (7):

$$(7) \quad \frac{F_v}{F_{v_o}}, \quad v \in V_{D-s}.$$

- Generate two independent random walks on V , started at v , using the transition probabilities (5). Let x and y be the leaf vertices at which the two walks are absorbed. There are four cases, whose frequencies will be estimated in Proposition 6.1.
 - (1) If $x \neq y$ and $\chi(x) = \chi(y)$, add this edge, and call it an **agreement edge**.
 - (2) If $\chi(x) \neq \chi(y)$, and either x or y (or both) are wild, then add this edge, and call it a **conflict edge**.
 - (3) If $x = y$, the result would be a **loop**, which is discarded.
 - (4) If $\chi(x) \neq \chi(y)$, and both x and y are tame, then this edge is discarded as **inadmissible**.

Multiple instances of the same edge may be created. The hidden ancestor graph is really a multigraph, but in practice we present it as a simple graph with integer edge weights, denoting the edge multiplicities.

4.3. Construction of the edges via matching. The following matching construction is statistically similar, though not exactly equivalent, to the random walks construction of Section 4.2. The differences are noted in Section 4.4.

Initialization: S_0, S_1, \dots, S_{D-1} are initialized to be empty lists. Here S_d will eventually contain half-edges corresponding to random walks starting at depth d from the root, terminating at a leaf.

Half-edge generation: For each $x \in L$, let (Y_1^x, \dots, Y_D^x) be a vector of independent Poisson random variables whose conditional mean, given the leaf marks, are

$$\mathbf{E}[Y_s^x] = q_s F_x.$$

Insert Y_s^x copies of the pair $(\pi^s(x), x)$ into the list $S_{D-s} \subset V_{D-s} \times L$. Such a pair is a surrogate for a random walk starting at the ancestor $\pi^s(x)$ and terminating at x . We may view this pair as a **half-edge**, where $r := \pi^s(x)$ at depth $D-s$ is viewed as the source of two random walks, one of which will terminate at x . We call r a **link node**. Repeat this procedure independently for all $x \in L$, so as to populate the sets S_0, S_1, \dots, S_{D-1} .

Random half-edge matching: For each j , the half-edges in S_j (or most of them) will be randomly matched up to form edges⁵. In practice, this means grouping by link node, shuffling the list at each link node, and then pairing up consecutive entries when allowed; see Algorithm 1 for formal details, where type refers to leaf node. For each fixed j , we are allowed to match $(r, x) \in S_j$ with $(r', x') \in S_j$ provided that the conditions

$$r = r'; \quad x \neq x'$$

hold. These conditions mean that x, x' are distinct leaf vertices for which r is a common ancestor⁶. Insert an edge $\{x, x'\}$ provided that the condition $\chi(x) = \chi(x')$, or the condition $\eta_x + \eta_{x'} > 0$, holds. In other words, either x and x' have the same tag, or else at least one of them is wild.

Matching failures: Some attempts will fail because they refer to the same leaf vertex (a loop⁷), and some will fail because the leaves have different labels, and yet neither is wild. A perfect matching is not expected. If the number of the half-edges in S_j with first component r is odd, then at least one half-edge is unmatched. By multiple rounds of Algorithm 1, we could try again to match half-edges which failed to be matched in the first round, to avoid loops or inadmissible edges. This has not been implemented.

4.4. How the matching construction compares with random walk pairs. Let us condition on the marks $\{F_x, x \in L\}$, and assume that a Poisson distribution is chosen whenever we have to generate the number of attempts, given its mean.

Distribution of half-edge counts: The number of times r , at height s , is sampled as a starting point in the *random walk construction* is a Poisson($q_s F_r / 2$) random variable; this fact follows from thinning a Poisson($F_{v_o} / 2$) random variable at rate $q_s F_r / F_{v_o}$. Of these starts, the chance that one walk of the pair reaches a leaf x descended from r is about $2F_x / F_r$. Overall,

⁵The construction is reminiscent of the well-known configuration model for constructing random graphs with a given degree sequence, as described in [7, Ch. 10].

⁶However r is not necessarily the lowest common ancestor, because two random walks, starting at r , and ending at x and y respectively, might agree for one or more steps before they diverge.

⁷Such matching failures in random graph constructions are examined in detail in Nordman et al [11].

Algorithm 1 Randomized multipartite matching: Given n items, each having one of $t \geq 2$ types, randomly partition most of the items into pairs whose types are different.

Require: An n -element set V , a map $T : V \rightarrow \{0, 1, 2, \dots, t-1\}$, and an initially empty set M of matched pairs

if $V = \emptyset$ or $|T(V)| = 1$ **then**
 Stop
else
 Set $U = \emptyset$ (receptacle to hold unmatched elements).
 Apply a uniform random permutation to V , giving x_0, x_1, \dots, x_{n-1} .
 for $(i = 0; i < (n-1)/2; i++)$ **do**
 if $T(x_{2i}) \neq T(x_{2i+1})$ **then**
 add $\{x_{2i}, x_{2i+1}\}$ to M
 else
 append x_{2i} and x_{2i+1} to U
 end if
 end for
 Set $V := U$ (prepare for the next round).
end if

the number of random walk pairs, started at r , where one walk reaches x , is approximately Poisson with a mean of $q_s F_x$, which is the product of $q_s F_r/2$ and $2F_x/F_r$. Likewise in the *matching construction*, a Poisson $q_s F_x$ number of half-edges, pointed at x , are created at r . Hence in this respect, the random walk construction and the matching construction are in agreement.

Unmatched half-edges versus loops: Two half-edges with the same link node r may fail to be matched because they point to the same leaf vertex, which is equivalent to failure of a pair of random walks, started at r , to create an edge because they terminate at the same leaf node. However there is an additional cause of failure unique to the matching construction: when there exist an odd number of half-edges at a link node, the odd one out cannot be matched. The expected number of lost edges due to odd numbers in the *matching* is $1/2$ the expected number of non-leaf nodes, i.e.

$$\frac{1}{2} \sum_{i=0}^{D-1} \mu^i = \frac{\mu^D - 1}{2(\mu - 1)},$$

where μ measures mean offspring in the latent tree. This comes to about $1/(2(\mu - 1))$ per leaf vertex.

Despite this caveat, we persevere in our abusive practice of generating the hidden ancestor graph in software via the efficient matching construction, while analyzing it via the random walks construction.

5. THE DEPTH ONE HIDDEN ANCESTOR GRAPH IN FULL DETAIL

Consider this section as a warm-up for Section 6.

5.1. Construction. In order to understand the rates of generating agreement edges and conflict edges in a hidden ancestor graph, let us begin with the almost trivial case where the *latent tree has depth one*, and the root node v_o has exactly $n \geq 2$ children. Each leaf node x :

- (1) Chooses to adopt the root's color according to a Bernoulli($1 - \rho$) trial, with all trials independent; otherwise it starts a new, unique color;
- (2) Chooses wildness according to a Bernoulli(ω) trial, with all trials independent;
- (3) Acquires a leaf mark F_x according to independent draws from a distribution with mean ν and variance η^2 . Here there is no dependency between mark and wildness: $\beta = 0$ in (3).

The notion of a pair of random walks reduces to *sampling two leaf nodes*, with replacement, where node x is sampled at rate F_x/F_{v_o} . We sample S times, where $S \sim \text{Binomial}(\sum_x F_x, \alpha/2)$, for some $\alpha \in (0, 1]$.

5.2. Statistics of the depth one case.

Lemma 5.1. *When the latent tree has depth one, and the hidden ancestor graph is parametrized as above, then the expected number of times that the two sampled leaves are different is*

$$(8) \quad M_E := \frac{\alpha\nu(n-1)}{2} \left(1 - \frac{\eta^2}{n\nu^2}\right) + O(n^{-2}).$$

(a) *The expected number of agreement multi-edges is*

$$(9) \quad M_A := (1 - \rho)^2 M_E.$$

(b) *The expected number of conflict multi-edges is*

$$(10) \quad M_C := \rho(2 - \rho)\omega(2 - \omega)M_E.$$

Remark: Observe that a high standard-deviation-to-mean ratio among the leaf marks reduces the number of edges created, especially when the offspring count n is moderate.

Numerical example: To aid the reader's intuition, consider a case where $n = 25$, $\alpha = 0.8$, $\nu = 14.0$, $\frac{\eta^2}{\nu^2} = 3.6$, $\rho = 0.1$, $\omega = 0.08$. Then $M_E = 114.8$, and we expect 93 agreement edges and 3 conflict edges among the 25 leaf vertices of this depth one hidden ancestor graph. About 25 edge attempts resulted in loops, and a further 19 failed because end points were tame, with different color labels. Overall the success rate was about 69%.

Proof. By the Remark (46) after Lemma A.1, the conditional expectation of the number K of times the two leaf nodes sampled are the same is

$$\mathbf{E}[K] = \frac{\alpha\nu}{2} + \frac{\alpha\eta^2}{2\nu} \left(1 - \frac{1}{n}\right) + O(n^{-2}).$$

Subtract this from the mean $n\alpha\nu/2$ of S to obtain (8). If the nodes differ, then an agreement edge is created if their labels agree; if labels do not agree, a conflict edge is created if at least one node is wild. The probability that two leaf nodes have the same label is $(1 - \rho)^2$. Multiply this by M_E to obtain (9). The event that two leaf nodes have different labels, and at least one is wild, has probability

$$(1 - (1 - \rho)^2)(1 - (1 - \omega)^2) = \rho(2 - \rho)\omega(2 - \omega)$$

which leads to formula (10) in a similar way. \square

6. DECOUPLING TIMES FOR PAIRS OF RANDOM WALKS

Estimating the numbers of agreement edges and conflict edges will depend on an analysis of the first step at which a pair of random walks, started at the same tree node, decouple from each other.

6.1. Assumptions about the latent tree. Let the random variable ξ_t denote the size of the t -th generation in the Galton-Watson tree. Assume the tree is supercritical (i.e. $\mu := \mathbf{E}[\xi_1] > 1$), and every non-leaf node in the tree has at least one child. It is well known that $(\mu^{-t}\xi_t)_{t \geq 0}$ is a non-negative martingale, and consequently

$$(11) \quad \mathbf{E}[\xi_t] = \mu^t.$$

Grimmett and Stirzaker [8, Ch. 5.4] express the variance $\zeta_t^2 := \text{Var}[\xi_t]$ in terms of $\text{Var}[\xi_1]$:

$$(12) \quad \zeta_t^2 = \frac{\zeta_1^2(\mu^t - 1)\mu^{t-1}}{\mu - 1}.$$

Introduce decreasing real parameters $\delta_t \in (0, 1)$ defined by

$$(13) \quad \delta_t = \mathbf{E}[1/\xi_t], \quad t = 0, 1, 2, \dots, D.$$

In particular, $\xi_0 = 1$ and so $\delta_0 = 1$. The second order Taylor expansion for δ_t is

$$\delta_t = \mu^{-t} + \mu^{-3t}\zeta_t^2 + O(\mu^{-t-2})$$

under suitable third moment assumptions.

We say that the offspring distribution is 1+Poisson($\mu - 1$) if $\xi_1 - 1$ is Poisson($\mu - 1$). Its mean is μ , and its variance is $\zeta_1^2 = \mu - 1$. This implies:

$$(14) \quad \zeta_t^2 = (\mu^t - 1)\mu^{t-1}; \quad \delta_t = \mu^{-t} + \mu^{-t-1} + O(\mu^{-t-2}).$$

6.2. Hitting probabilities of random walk on the tree. Our larger goal is to select parameters for a hidden ancestor graph, so that a simulated graph will have statistical characteristics similar to those of a large graph we wish to model. The first step will be to derive formulas which express measurable quantities in terms of hidden ancestor graph parameters. We begin with analysis of the random walks introduced in Section 4.2.

Lemma 6.1.

- (a) *The random walk (X_t) started at node $X_0 := v \in V$ terminates at leaf node $x \in L(v)$ with probability F_x/F_v .*
- (b) *Fix any $d \in \{0, 1, 2, \dots, D-1\}$, and start the random walk at some $v \in V_d$ selected according to the distribution (7); the walk terminates at leaf node $x \in L$ with probability F_x/F_{v_o} , not depending on d .*
- (c) *The probability that the vertex label $\chi(x)$ coincides with the vertex label $\chi(v)$ is*

$$(15) \quad \prod_{j=d+1}^D (1 - \rho_j)$$

where ρ_j was defined in (2).

Proof. The first assertion is clear from the definition when $\pi(x) = v$. In general it follows by induction on the depth d of x with respect to v , since telescoping occurs when multiplying probabilities such as

$$p_{v^{(0)}, v^{(1)}} p_{v^{(1)}, v^{(2)}} \cdots p_{v^{(d-1)}, v^{(d)}}.$$

As for the second, the chance that $x \in L$ is the terminal state is

$$\sum_{v \in V_d} \frac{F_v}{F_{v_o}} \cdot \frac{F_x}{F_v} 1_{\{x \in L(v)\}}$$

which simplifies to F_x/F_{v_o} , because there is only one v which gives a non-zero contribution to the sum. The formula (15) follows from the independence of the choices to adopt the parent's tag, along each step of the path from v to x . \square

6.3. Decoupling estimates. For $0 \leq t < s \leq D$, let $H_{s,t}$ count the pairs of random walks which begin at height $s \geq 1$ and remain coupled at height $t < s$. For example, $H_{s,0}$ counts pairs which lead to loops in the hidden ancestor graph edge construction, and are rejected. The total number of pairs of random walks which start at height s is written as $H_{s,s}$, and may be decomposed as

$$H_{s,s} = H_{s,0} + \sum_{t=1}^s \Delta_{s,t-1}$$

where $\Delta_{s,t-1} := H_{s,t} - H_{s,t-1}$, for $t = 1, 2, \dots, s$. Thus $\Delta_{s,t}$ counts the pairs of random walks, starting at height s , whose first decoupling occurs at height t . Estimating the means of $(\Delta_{s,t})_{0 \leq t < s \leq D}$ will be the key to estimating the number of agreement edges and conflict edges in the hidden ancestor graph. It suffices to estimate $\mathbf{E}[H_{s,t}]$, for $0 \leq t < s \leq D$, since we know

$$(16) \quad \mathbf{E}[H_{s,s}] = \mathbf{E}[\mathbf{E}[H_{s,s} \mid F_{v_o}]] = \mathbf{E}[q_s F_{v_o}/2] = \frac{q_s \nu \mu^D}{2}$$

when leaf marks have mean ν .

Recall from (11) and (12) that ξ_t has mean μ^t and variance ζ_t^2 . The following observation is elementary.

Lemma 6.2. *Let Y denote the sum of ξ_t independent copies of a random variable with mean ν and variance η^2 . Then*

$$(17) \quad \mathbf{E}[Y] = \nu \mu^t; \quad \text{Var}[Y] = \eta^2 \mu^t + \nu^2 \zeta_t^2.$$

Lemma 6.3. *Assume leaf marks have mean ν , variance η^2 , and finite third moments. Also assume the offspring distribution in the latent tree has mean $\mu > 1$, variance ζ_1^2 , and has no mass at zero. For any $0 \leq t < s \leq D$, the expected number of pairs of random walks which begin at height $s \geq 1$ and remain coupled at height $t < s$, is*

$$\mathbf{E}[H_{s,t}] = q_s \mu^D h_{s,t} + O(\mu^{D-3s+2t}),$$

where

$$(18) \quad a := \frac{\eta^2}{\nu}; \quad b := \frac{\nu \zeta_1^2}{\mu(\mu-1)}; \quad h_{s,t} := \frac{1}{2} \left(\frac{\nu}{\mu^{s-t}} + (1 - \delta_{s-t}) \frac{a + b(\mu^t - 1)}{\mu^s} \right).$$

The formula $\mathbf{E}[H_{s,s}] = q_s \mu^D h_{s,s}$ is exactly valid, with $h_{s,s} = \nu/2$.

Remarks:

(a) Suppose the latent tree is deterministic, and the leaf marks are identical and non-random. Then $\eta^2 = 0$ and $\zeta_1^2 = 0$, so

$$\mathbf{E}[H_{s,t}] = \frac{\nu q_s \mu^{D-(s-t)}}{2}.$$

This makes sense because $(\nu q_s \mu^D/2)$ is the expected number of pairs of random walks which start at height s . Each such pair has probability $\mu^{-(s-t)}$ of remaining coupled for $s-t$ steps.

(b) A common choice for the distribution of offspring is to take $\xi_1 - 1$ to be Poisson($\mu - 1$), giving a mean of μ and a variance $\zeta_1^2 = \mu - 1$. When $t = 1$, the value of $2\mu^s h_{s,1}$ is

$$\nu\mu + (1 - \delta_{s-1}) \left(\frac{\eta^2}{\nu} + \frac{\nu(\mu - 1)}{\mu} \right).$$

This illustrates that the variance η^2 of the leaf marks exerts a significant effect.

(c) In the case $t = 0$, the value of $2\mu^s h_{s,0}$ is $\nu + (1 - \delta_s)\eta^2/\nu$. It follows that the expected number of loops, i.e. pairs of random walks which never decouple is

$$(19) \quad M_L := \sum_{s=1}^D \frac{q_s \mu^{D-s}}{2} \left(\nu + (1 - \delta_s) \frac{\eta^2}{\nu} \right).$$

Here the variance η^2 of the leaf marks exerts an even greater effect.

Proof. Fix a specific height s vertex v . The number of pairs of random walks started at v , denoted $H_{s,s}^v$, has conditional mean

$$\mathbf{E}[H_{s,s}^v \mid \mathcal{F}_{D-s}] = \frac{q_s F_v}{2}.$$

Let $H_{s,t}^v$ denote the number of pairs of random walks, started at v , which remain coupled at height $t < s$. Condition on the number ξ_{s-t} of offspring of v in generation $s-t$. When $\xi_{s-t} = n$, let v_1, v_2, \dots, v_n denote the nodes descended from v , at height t . It follows implicitly from Lemma 6.1 that the marks F_{v_1}, \dots, F_{v_n} on these nodes are i.i.d. random variables, with

$$\sum_{i=1}^n F_{v_i} = F_v.$$

Their mean and variance are given by (17) in Lemma 6.2:

$$\nu_t := \mathbf{E}[F_{v_i}] = \nu \mu^t; \quad \eta_t^2 := \text{Var}[F_{v_i}] = \eta^2 \mu^t + \nu^2 \zeta_t^2.$$

The moment assumptions on the leaf marks mean that Lemma A.1 applies. The simplified version (46) of that Lemma, with $\alpha = q_s$, estimates weighted sampling collisions as:

$$\mathbf{E}[H_{s,t}^v \mid \xi_{s-t} = n] = \frac{q_s}{2} \left(\nu_t + \frac{\eta_t^2}{\nu_t} \left(1 - \frac{1}{n} \right) \right) + O(n^{-2}).$$

Undo the conditioning on $\xi_{s-t} = n$, using (13), noting that $\xi_{s-t} = O(\mu^{s-t})$, to obtain:

$$\mathbf{E}[H_{s,t}^v] = \frac{q_s}{2} \left(\nu_t + \frac{\eta_t^2}{\nu_t} (1 - \delta_{s-t}) \right) + O(\mu^{-2(s-t)}).$$

Using the formula for ζ_t^2 in (12), the variance to mean ratio may be written in terms of the constants a, b from (18) as:

$$\frac{\eta_t^2}{\nu_t} = \frac{\eta^2}{\nu} + \frac{\nu\zeta_t^2}{\mu^t} = \frac{\eta^2}{\nu} + \frac{\nu\zeta_1^2(\mu^t - 1)}{\mu(\mu - 1)} = a + b(\mu^t - 1).$$

Combine the formulas to obtain:

$$\mathbf{E}[H_{s,t}^v] = \frac{q_s}{2} (\nu\mu^t + (1 - \delta_{s-t}) (a + b(\mu^t - 1))) + O(\mu^{-2(s-t)}).$$

The number of choices of v at height s is a random variable with a mean of μ^{D-s} . The collision count $H_{s,t}^v$ at v has the same distribution for all choices of v . Hence $\mathbf{E}[H_{s,t}]$ is obtained by multiplying $\mathbf{E}[H_{s,t}^v]$ by μ^{D-s} . Since $1 - \delta_0$ is zero, the formula is exactly valid when $s = t$, by (16). \square

6.4. Agreement edge and conflict edge estimates. Recall that the number of pairs of random walks initiated at a specific tree node v at height $s \geq 1$ is an integer random variable Q_v , with conditional mean $q_s F_v/2$, given \mathcal{F}_{D-s} . Such pairs of random walks fall into two classes:

- (i) Those which never decouple. We estimated these, for all s , and all v at height s , in (19).
- (ii) Those which decouple at some height $t < s$, with last common ancestor $u \in V_{D-t-1}$. An agreement multi-edge results precisely when the color label of u is maintained at every step along both walks. Squaring (15) shows that this event has probability

$$(20) \quad A_t := \prod_{d=D-t}^D (1 - \rho_d)^2.$$

Here A_t is the chance that two random walks, which first decouple at height t , travel along paths all of whose nodes inherit the color of their parent. Otherwise a conflict multi-edge results if at least one color label changes along this pair of walks, and at least one terminal state is wild, an event with probability

$$(21) \quad C_t := (1 - A_t)\omega(2 - \omega).$$

Proposition 6.1. (a) *The expected number of pairs of random walks whose first decoupling occurs at height t is approximated up to $O(\mu^{D-t-3})$ by $\mu^D \Gamma_t$, where*

$$(22) \quad \Gamma_t := \sum_{s=t+1}^D q_s (h_{s,t+1} - h_{s,t}),$$

using the precomputed array $(h_{s,t})_{s \geq t}$ given in (18).

- (b) *The expected number of agreement multi-edges in the hidden ancestor graph is*

$$M_A := \mu^D \sum_{t=0}^{D-1} \Gamma_t A_t + O(\mu^{D-3}),$$

for A_t as in (20).

(c) The expected number of conflict multi-edges in the hidden ancestor graph is

$$M_C := \mu^D \sum_{t=0}^{D-1} \Gamma_t C_t + O(\mu^{D-3}),$$

for C_t as in (21).

Remark 6.1. Call an edge $\{x, y\}$ a **sibling edge** if x and y are leaves with the same parent. Proposition 6.1 shows that the proportion of all agreement multi-edges which are sibling multi-edges is

$$(23) \quad \pi'_1 := \frac{\Gamma_0 A_0}{\Gamma \cdot A}; \quad \Gamma \cdot A := \sum_{t=0}^{D-1} \Gamma_t A_t.$$

The **mean vertex multi-degree** in the agreement, and conflict graph, respectively, are:

$$(24) \quad d'_A := 2 \Gamma \cdot A; \quad d'_C := 2\omega(2 - \omega) \Gamma \cdot (\mathbf{1} - A) = 2 \sum_{t=0}^{D-1} \Gamma_t C_t.$$

Proof. By our previous discussion, the expected number of pairs of random walks whose first decoupling occurs at height t is

$$\sum_{s=t+1}^D \mathbf{E}[\Delta_{s,t}], \quad t = 0, 1, \dots, D-1,$$

where $\Delta_{s,t} := H_{s,t+1} - H_{s,t}$. Apply the estimate in Lemma 6.3 in the form

$$\mathbf{E}[H_{t+1,t+1}] = q_{t+1} \mu^D h_{t+1,t+1},$$

where the last expression is exact, while for $s > t$,

$$\mathbf{E}[H_{s,t}] = q_s \mu^D h_{s,t} + O(\mu^{D-3s+2t}).$$

It follows that, up to an $O(\mu^{D-t-3})$ error,

$$\sum_{s=t+1}^D \mathbf{E}[H_{s,t+1} - H_{s,t}] = \mu^D \sum_{s=t+1}^D q_s (h_{s,t+1} - h_{s,t}) = \mu^D \Gamma_t.$$

The error estimate arises because $D - 3s + 2t \leq D - t - 3$ when $s \geq t + 1$.

The remainder of the proof follows the reasoning surrounding the introduction of A_t and C_t in (20) and (21), respectively. This machinery works because color choices are independent of the tree and of the marks, and every node has at least one child. In particular

$$M_A := \mu^D \sum_{t=0}^{D-1} \Gamma_t A_t + O(\mu^{D-3}),$$

and similarly for M_C . □

As a check on the correctness of the formulas, consider constant leaf marks and a deterministic μ -ary tree. Here randomness persists only in the color labelling of tree nodes, and in the random walks for constructing edges.

Corollary 6.1. *Suppose the offspring distribution and the leaf marks both have variance zero, so $h_{s,t} = \nu/(2\mu^{s-t})$ in (18). Then the estimates of Proposition 6.1 take the simpler, exact form:*

$$M_A = \frac{\nu\mu^D(\mu-1)}{2} \sum_{s=1}^D q_s \mu^{-s} \sum_{t=0}^{s-1} A_t \mu^t; \quad M_C = \frac{\nu\mu^D(\mu-1)}{2} \sum_{s=1}^D q_s \mu^{-s} \sum_{t=0}^{s-1} C_t \mu^t.$$

Proof. The formula for $h_{s,t+1} - h_{s,t}$ now becomes exactly

$$h_{s,t+1} - h_{s,t} = \frac{\nu\mu^{-s}}{2} (\mu^{t+1} - \mu^t).$$

Substitute this into the formula for M_A to obtain:

$$M_A := \sum_{t=0}^{D-1} \Gamma_t A_t = \frac{\nu\mu^D}{2} \sum_{s=1}^D q_s \mu^{-s} \sum_{t=0}^{s-1} A_t \mu^t (\mu - 1).$$

Likewise on replacing A_t by C_t . □

7. MEAN CLUSTERING IN THE AGREEMENT GRAPH

7.1. Average local clustering coefficient.

Definition 7.1. *The **average local clustering coefficient** (ALCC) of a finite simple graph $G := (V, E)$, is the mean $\mathbf{E}[W]$ of a $\{0, 1\}$ -valued random variable W , derived as follows. Sample a vertex uniformly at random, say $v \in V$. (a) If v has degree less than two, then $W = 0$. (b) Otherwise, sample two of the neighbors of v uniformly at random without replacement, say v', v'' , and take W to be the indicator of the event $\{\{v', v''\} \in E\}$.*

This section takes a minimal approach to estimating clustering. In particular, we ignore the possibility (a) in the definition, and focus on (b). A more elaborate model is in preparation [3].

7.2. Sibling subgraph. For a leaf vertex x , the **siblings** of x consist of those $\xi - 1$ leaves y with the same parent as x , i.e. $\pi(x) = \pi(y)$. As before, mean offspring per node in the latent tree is $\mathbf{E}[\xi] = \mu$. The set of ξ vertices, consisting of x and its siblings, induces a subgraph of the hidden ancestor graph which we call x 's **sibling subgraph**. Edges between any pair of siblings, called **sibling edges**, are necessarily agreement edges, under our assumption that $\rho_D = 0$, since they all carry the same tag.

Our discussion of mean clustering is restricted to the agreement graph, where nearly all clustering happens in cases of interest. Having sampled a vertex x , we further limit ourselves to estimating mean clustering in the sibling subgraph of x . Proceed using the following clustering heuristic:

Nearly all clustering in the hidden ancestor graph occurs in sibling subgraphs.

In other words, we neglect the low probability event of triangles among non-siblings. The random overlapping communities model of Petti and Vempala [12] shows similar behavior, where dense communities play a role analogous to sibling subgraphs.

The mean vertex multi-degree d'_A in the agreement graph was estimated in (24), and the proportion π'_1 of all agreement multi-edges which are sibling multi-edges was estimated in (23). This means that the mean vertex multi-degree in the restriction of the agreement graph to a sibling subgraph is $\pi'_1 d'_A$. Hence the sibling subgraph has about $\mu \pi'_1 d'_A / 2$ multi-edges, distributed among about $\mu(\mu-1)/2$ possible edge positions. Using a Poisson approximation, this implies that the probability that two siblings are actually adjacent is about

$$(25) \quad 1 - e^{-\pi'_1 d'_A / (\mu-1)}.$$

The effect on ALCC of the variance of the leaf marks will be ignored here, but is studied in detail in [3].

7.3. Mean vertex degree. The clustering heuristic goes hand in hand with the duplicate edge heuristic:

Nearly all duplicate multi-edges in the hidden ancestor graph occur in sibling subgraphs.

This heuristic, combined with (23), (24), and (25), imply that the mean d_A of the number of distinct neighbors in the agreement graph, assuming that non-sibling edges are seldom duplicated, is

$$(26) \quad d_A = (1 - \pi'_1) d'_A + d_S; \quad d_S := (\mu - 1)(1 - e^{-\pi'_1 d'_A / (\mu-1)}).$$

Here d_S stands for the mean number of distinct neighbors in the sibling subgraph, which is $(\mu - 1)$ times the edge probability (25). Implicit in (26) is the formula for π_1 , which is the probability that a neighbor in the agreement graph is a sibling neighbor:

$$(27) \quad \pi_1 = \frac{d_S}{d_A} = \frac{d_S}{(1 - \pi'_1) d'_A + d_S}.$$

The duplicate edge heuristic also implies that duplicate edges hardly ever happen in the conflict graph, since sibling edges cannot be conflict edges when $\rho_D = 0$. Thus we may equate mean conflict degree d_C with mean conflict multi-degree d'_C , defined in (24).

7.4. Mean clustering coefficient heuristic. Under these assumptions, we claim the mean clustering coefficient κ in the agreement graph has a crude approximation in terms of μ , d'_A , π'_1 , and π_1 :

$$(28) \quad \kappa \approx \pi_1^2 (1 - e^{-\pi'_1 d'_A / (\mu-1)}).$$

Justification for (28): Sample a leaf vertex x , and assume y, z are two neighbors of x in the agreement graph, selected uniformly at random. Denote by $\Delta_{y,z}^x$ the event that both $\{x, y\}$ and $\{x, z\}$ are sibling edges, which has conditional probability π_1^2 , given the last sentence. Since the sibling relation is transitive, y and z are siblings if $\Delta_{y,z}^x$ occurs. Since $\rho_D = 0$, we already know x, y, z all carry the same tag. Hence the mean clustering coefficient is $\mathbf{P}[\Delta_{y,z}^x]$ times the probability that y and z are adjacent, which we estimated in (25). Hence the formula (28).

8. COLOR CHANGE PARAMETER

8.1. Number of nodes in the latent tree. As usual, the latent tree is a supercritical Galton-Watson tree (V, T) , of depth D , where every non-leaf node has at least one child, and so all leaves are at depth D . Vertices of the Galton-Watson tree can be partitioned as

$$V := V_0 \cup V_1 \cup \cdots \cup V_D$$

where $V_0 := \{v_o\}$ and V_d denotes the vertices at depth d from the root v_o . Take $\xi_d := |V_d|$ to be the number of offspring in the d -th generation, as before. It follows from (11) that the expected number of vertices at depth d is μ^d , and the total mean is

$$(29) \quad \mathbf{E}[|V|] = \sum_{d=0}^D \mu^d = \frac{\mu^{D+1} - 1}{\mu - 1}.$$

8.2. Expected number of distinct labels.

Lemma 8.1. *The expected number of distinct labels of vertices in a depth D Galton-Watson tree with mean offspring $\mu > 1$, and with rate (2) of new label generation, is*

$$(30) \quad K(\mu, D, \theta) := 1 + \theta(\mu - 1) \sum_{d=1}^{D-1} \frac{1}{1 + (\theta\mu - \theta - \mu)\mu^{-d}}.$$

Remark: For $\theta(\mu - 1) > 1$, which is typical in our models, (30) is bounded above by $\theta(\mu - 1)(D - 1)$, which is logarithmic in the number of vertices, and linear in θ . The bound $\theta > \frac{K-1}{(D-1)(\mu-1)}$ follows. If μ and θ are fixed, K is roughly proportional to the log of the number of leaf vertices. Hence if a graph with n vertices is replaced by a miniature model with ϵn vertices, the number of distinct labels in the miniature model, divided by the number of labels in the original, should be about $\log(\epsilon n)/\log n$ in order to preserve local structure.

Proof. The mean number of vertices at depth d is μ^d . By (2), the expected number of fresh labels introduced by vertices at depth d is

$$\frac{\theta(\mu - 1)\mu^d}{(\theta - 1)(\mu - 1) + \mu^d - 1}.$$

Finally sum over d from 1 to $D - 1$. □

9. FITTING A MODEL WITH HIGH CLUSTERING COEFFICIENT

9.1. Input data.

Assume that we are given

- (1) An estimate κ of the average local clustering coefficient in the agreement graph. For example $\kappa = 0.51$.
- (2) Estimates d_A and d_C of the mean of the vertex degree distribution in the agreement graph and conflict graph, respectively. For example 15.0 and 1.5.
- (3) The number of distinct labels we expect to see among the leaves of the Galton-Watson tree; for example 250.
- (4) An estimate η^2 of the variance of the vertex degree distribution for the union of the agreement and conflict edges; for example 500.
- (5) An upper bound for the desired vertex count. For example 3×10^7 .

Our goal will be to select the six parameters listed in the bottom row of Table 1, so that we may synthesize a hidden ancestor graph with the desired statistical properties. This section will explain a simple trick to convert what seems like a complicated nonlinear six-parameter fitting problem into a pair of nested one-dimensional searches, through values of parameters q_1 and ν , respectively.

9.2. A simplified fit: the cube root principle. Recall our estimate (28) for the average local clustering coefficient:

$$\kappa \approx \pi_1^2 (1 - e^{-\pi_1' d_A' / (\mu-1)}).$$

The right side is the square of the probability π_1 that an agreement edge is a sibling edge, times the chance that two arbitrary siblings are adjacent in the agreement graph. To simplify, we satisfy (28) by the special choice we call the **cube root principle**, which equates the probability that an agreement edge is a sibling edge with the probability that two siblings are adjacent:

$$(31) \quad \pi_1 = \kappa^{1/3}; \quad 1 - e^{-\pi_1' d_A' / (\mu-1)} = \kappa^{1/3}.$$

In effect, this constraint restricts us to fitting a sub-model of the hidden ancestor graph, for which parameter selection is especially easy .

Lemma 9.1. *Under the cube root principle (31), the mean offspring μ satisfies*

$$(32) \quad \mu = 1 + d_A,$$

the mean agreement multi-degree satisfies

$$(33) \quad d_A' = d_A (1 - \kappa^{1/3} - \log(1 - \kappa^{1/3})),$$

and the proportion of agreement multi-edges which are sibling multi-edges is

$$(34) \quad \pi_1' = \left(1 - \frac{1 - \kappa^{1/3}}{\log(1 - \kappa^{1/3})} \right)^{-1}$$

all of which are computable in terms of observables κ and d_A .

Proof. The cube root principle (31) may be combined with the formula (26) for d_S :

$$(\mu - 1)(1 - e^{-\pi_1' d_A' / (\mu-1)}) = (\mu - 1)\kappa^{1/3} = d_S = \pi_1 d_A = \kappa^{1/3} d_A,$$

which implies (32). Rewrite the second identity in (31) with d_A' as the subject, to obtain:

$$d_A' = \frac{-(\mu - 1) \log(1 - \kappa^{1/3})}{\pi_1'} = \frac{-d_A \log(1 - \kappa^{1/3})}{\pi_1'}.$$

However it is also true by (26) that

$$d_A = (1 - \pi_1') d_A' + d_S = (1 - \pi_1') d_A' + \pi_1 d_A,$$

Combine the previous two lines to give:

$$\frac{1 - \pi_1}{1 - \pi_1'} = \frac{d_A'}{d_A} = \frac{-\log(1 - \kappa^{1/3})}{\pi_1'}.$$

Substitute for π_1 from (31), and solve for $1/\pi_1'$ to give (34):

$$\frac{1}{\pi_1'} = 1 + \frac{1 - \kappa^{1/3}}{-\log(1 - \kappa^{1/3})}.$$

The last two expressions combine to give formula (33) for d'_A :

$$d'_A = \frac{-d_A \log(1 - \kappa^{1/3})}{\pi'_1} = d_A (1 - \kappa^{1/3} - \log(1 - \kappa^{1/3})).$$

□

For example $d_A = 25.0$ and $\kappa = 0.5$ give $\mu = 26.0$, $d'_A = 44.6181$.

9.3. Choice of depth. Given an upper bound $|V|$ on the number of vertices in the model, fix the tree depth D to be $\lfloor \log |V| / \log \mu \rfloor$, assuming the latter is at least 3. If the fitting procedure fails later on, go back and increase $|V|$ and D .

9.4. Color change rate. Knowing μ, D and the number of colors, we can choose a value for θ to fit (30). This allows all the (ρ_d) to be specified, subject to $\rho_1 = 1$ and $\rho_D = 0$. Hence we also know the coefficients (A_t) defined in (20).

9.5. One-parameter model for height distribution. Simplify by restricting the law of the height \mathcal{H} to be a mixture of an atom at 1, and a uniform distribution on heights 2 to D :

$$(35) \quad q_1 \in [0, 1); \quad q_s := \frac{1 - q_1}{D - 1}; \quad 2 \leq s \leq D.$$

9.6. Exploring the height distribution. Adopt the 1+Poisson($\mu - 1$) offspring distribution. The parametrization (14) is now available, and the $(h_{s,t})$ matrix can be computed using (18) for any choice of the (q_s) , as a function of ν . The formulas also involve η^2 , for which we accept the proposed estimate.

Decrement q_1 by small amounts, starting at $q_1 = 1$, and compute (q_s) according to (35). For each choice of q_1 , increase the value of ν , starting from $\nu = d'_A$, until the mean agreement multi-degree (24), based on (18), falls into agreement with d'_A . Denote by $\nu(q_1)$ this value of ν , shown on the left side of Figure 5. This choice of ν is valid only if (31) also holds, which requires

$$(36) \quad \pi'_1 := \frac{2\Gamma_0 A_0}{d'_A} = \left(1 - \frac{1 - \kappa^{1/3}}{\log(1 - \kappa^{1/3})}\right)^{-1}$$

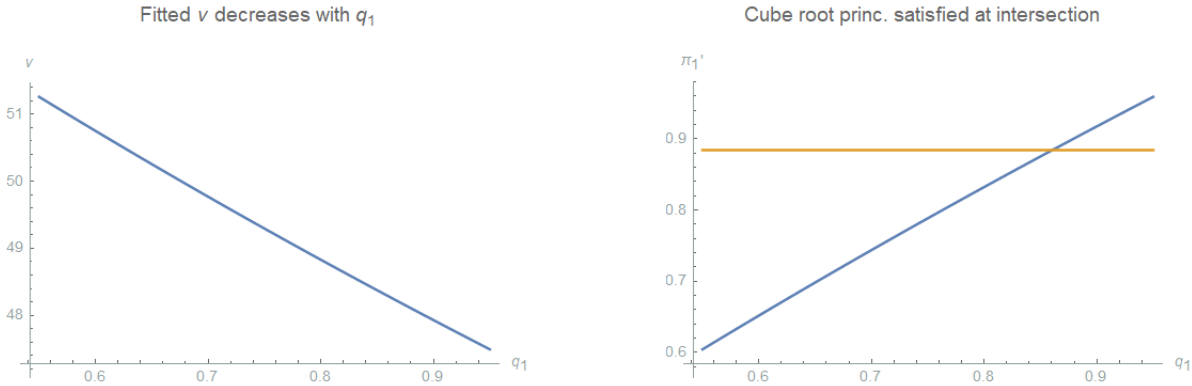
using formulas (23), (24), and (34), where Γ_0 depends on ν via the $(h_{s,t})$ matrix. For $q_1 \approx 1$, π'_1 will also be close to 1 (i.e. nearly all agreement edges are sibling edges), which means that π'_1 exceeds the right hand side of (36). However as q_1 decreases, more pairs of random walks start higher in the latent tree, and π'_1 also decreases. This monotonicity, illustrated on the right side of Figure 5, supports the notion that there is a unique solution, if one exists.

Having found the pair $(q_1, \nu(q_1))$ for which (36) holds and d'_A is correct, we know the mean number of proposed edges whose end points have different colors. If this exceeds the number of conflict edges, we can fit $\omega < 1$ to give the desired number of conflict edges, using the formula (24) for the known mean conflict degree $d_C = d'_C$, namely

$$1 - \omega = \sqrt{\left(1 - \frac{d_C}{2\Gamma \cdot (1 - A)}\right)}$$

Otherwise go back to Section 9.3 and increase D by 1.

FIGURE 5. **Fitting hidden ancestor graph parameters:** *Left:* As q_1 decreases, the required value of ν increases to compensate for loss of agreement edges. *Right:* As q_1 increases, the proportion π'_1 of sibling multi-edges increases. The horizontal line shows the desired value (34) for π'_1 , under the cube root principle. The intersection determines the fitted value $q_1 = 0.861$, when $\pi'_1 = 0.884$.



9.7. Summary and concrete examples. In summary, we move along a curve $(q_1, \nu(q_1))$ where q_1 is decreased from 1.0, and $\nu(q_1)$ is increased, while μ and D remain the same, stopping when the ratio of sibling edges to agreement edges drops to the cube root of the ALCC. More agreement edges coming from pairs of random walks from heights greater than 1 compensate for fewer sibling edges, keeping agreement edge counts the same, but adding greater numbers of proposed edges whose end points have different colors. For a suitable value of ω , a proportion of these will become conflict edges.

Table 1 offers a specific example of this fitting procedure. The modelling target is a graph of 30M vertices and nearly 400M edges. Both a 1% and a 37% scale hidden ancestor graph were built, in about fifteen seconds and six minutes, respectively⁸. The matching of half-edges took three quarters of the time. For the last row, 557M half-edges were produced, of which 8% were lost in the matching; after de-duplicating sibling multi-edges, 136M distinct edges remained. With depths of 4 and 5 respectively, the fitted parameters of the two models differ somewhat. For example, about 4% of vertices are wild in the smaller graph, and 7% in the larger one.

The models match the target in an acceptable way, except that the variance in vertex degree was not as large as intended. This reflects the absence of vertices of extremely high degree, which occurred in the target graph. The variance in the degree distribution is further reduced in small scale models. Other statistics of generated graphs typically deviate by 0 – 10% from those of the target. We attribute this to sampling variance in graph generation, and to crude approximations used in the parameter derivations.

⁸Running JDK 14 on Intel Xeon E5-2669, 56 cores. JGraphT [6] used for graph manipulation.

TABLE 1. *The Inputs row shows values of six observable quantities in a graph we wish to model. Two Hidden Ancestor Graph instances, at scales of 1% and 37% respectively, were built using the parameters shown in the last seven columns. The 1% Sim. and 37% Sim. rows report their statistical features. Note the poor fit in the η^2 column.*

	$ V $	K	d_A	d_C	κ	η^2	μ	D	θ	q_1	μ_o	σ_o	ω
Inputs	30M	200	25.0	0.3	0.5	700	-	-	-	-	-	-	
1% Sim.	326K	186	23.5	0.37	0.48	70	26	4	3.62	0.82	3.79	0.495	0.043
37% Sim.	11M	204	23.6	0.36	0.47	74	26	5	2.34	0.85	3.76	0.51	0.075

10. IMPLEMENTATION OF THE HIDDEN ANCESTOR GRAPH

10.1. Hidden ancestor graph software. The construction described in Sections 2, 3, and 4 have been implemented in Java software, capable of producing hidden ancestor graph instances with over a hundred million edges. One such instance is described in the last line of Table 1. The code performs the following functions:

- (1) Read a set of input statistics, as in the second line of Table 1, and compute fitted parameters, as in the third line of Table 1. Typically we will generate a synthetic graph with one to twenty percent of the number of vertices of the original, but with similar statistical structure in the neighborhood of a typical vertex.
- (2) Generate the Galton-Watson tree, node labels, and wildness tags.
- (3) Generate random leaf marks from the log-normal(μ_o, σ_o) distribution, with parameters μ_o, σ_o computed in (41) below.
- (4) Generate the hidden ancestor graph edges via the matching method of Section 4.3.
- (5) Insert the multi-edges into a weighted graph data structure, and separate the agreement graph and conflict graph.
- (6) Diagnose the statistical properties of the agreement graph and conflict graph, and compare them to the input statistics.

10.2. Vertex degree distribution: the log-normal option. Clauset, Shalizi, & Newman [2] have examined heavy tailed distributions in large networks, in the attempt to detect true power-law distributions. Mitzenmacher [10] surveys generative models for power-law and log-normal distributions. For the network traffic data we have studied, log-normal is a better fit than Zipf (power-law) to the vertex degree distribution. Moreover our analysis of the random walks in Lemma 6.3 makes finite third moment assumptions on the leaf marks, which place a lower bound on the exponent in a Zipf law. These assumptions are valid for any log-normal distribution, since all log-normal moments are finite. Indeed the relationship between log-normal(μ, σ) parameters and the mean ν and variance η^2 is:

$$(37) \quad \nu = e^{\mu + \sigma^2/2}; \quad \eta^2 = \nu^2(e^{\sigma^2} - 1).$$

We shall now describe how to proceed with a log-normal model.

10.3. Maximum likelihood for the log-normal. Recall that, in fitting the hidden ancestor graph, the parameter ν (mean of the leaf marks) is fitted as in Figure 5, whereas the parameter η^2 (variance of the leaf marks) is taken straight from the vertex degree distribution

of the graph we wish to model. The simple way to do this leads to bias, but we describe it first for the sake of clarity.

Simplistic approach: Suppose y_1, y_2, \dots, y_n are the logs of the vertex degrees in a graph we wish to model. Fit a $\text{Normal}(\mu, \sigma^2)$ distribution to the (y_i) using maximum likelihood estimates (MLE) $\hat{\mu}$ and $\hat{\sigma}$:

$$(38) \quad \hat{\mu} := \bar{y} := \frac{1}{n} \sum_{i=1}^n y_i; \quad \hat{\sigma} := \sqrt{\left(\frac{1}{n} \sum_{i=1}^n (y_i - \bar{y})^2 \right)}.$$

Compute η^2 by substituting $(\hat{\mu}, \hat{\sigma})$ into (37): $e^{2\hat{\mu} + \hat{\sigma}^2} (e^{\hat{\sigma}^2} - 1)$.

Low-bias approach: The drawback of the simplistic approach is that $e^{\hat{\mu} + \hat{\sigma}^2/2}$ is a biased estimate of ν . A bias-reducing option is a constrained MLE, in which the expected mean vertex degree coincides with the actual mean, which we denote by e^φ :

$$(39) \quad e^\varphi := \frac{1}{n} \sum_{i=1}^n e^{y_i}$$

whose expected value is $e^{\mu + \sigma^2/2}$. Our preferred choice for η^2 when setting model parameters will be

$$(40) \quad \eta^2 = e^{2\varphi} (e^\tau - 1); \quad \tau = 2(\sqrt{(\hat{\sigma}^2 + (\varphi - \bar{y})^2 + 1)} - 1).$$

The quantity τ is a constrained MLE for σ^2 , derived in the Appendix, Lemma B.1.

10.4. Practical steps for a hidden ancestor graph with log-normal leaf marks. During the model fitting procedure described in Section 9, we derive a value for the mean ν of the leaf marks, based on the choice (40) for η^2 . When we need to generate log-normal leaf marks, we select parameters (μ_o, σ_o) so that $\text{log-normal}(\mu_o, \sigma_o)$ has mean ν and variance η^2 according to (37), i.e.

$$(41) \quad \sigma_o^2 = \log(1 + \eta^2/\nu^2); \quad \mu_o = \log \nu - \frac{\sigma_o^2}{2}.$$

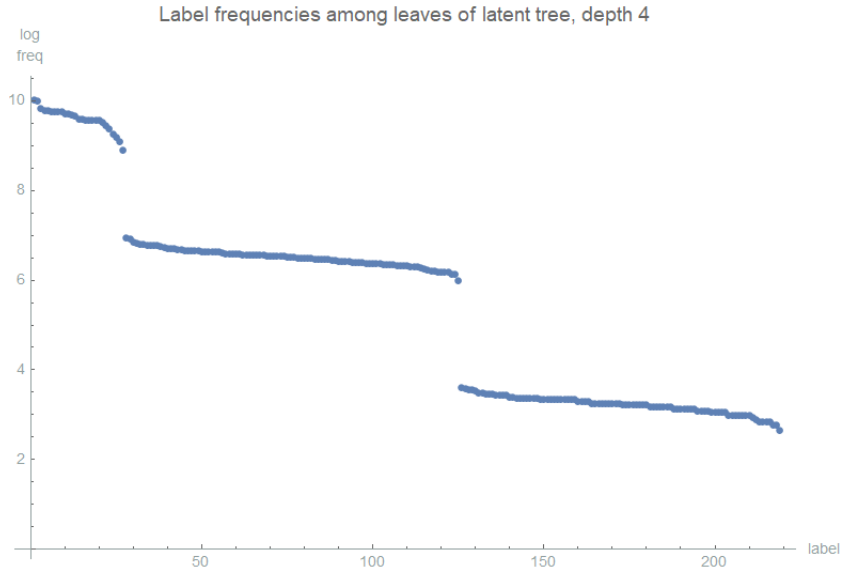
11. FUTURE WORK: LABEL FREQUENCIES IN THE AGREEMENT GRAPH

11.1. Label frequency fitting problem. Our approach to fitting the hidden ancestor graph has been crude, inasmuch as we have made no effort to fit the label frequencies among leaf nodes of the latent tree. Indeed by making the color change parameter depend only on depth, the label frequencies arising from a latent tree of depth D typically fall into $D - 1$ clusters, depending on the depth of the tree node at which the label originated. See Figure 6 for an illustration of three clusters of frequencies when the latent tree has depth four. The highest frequencies are associated with labels originating among the children of the root, and the lowest among those originating among the parents of the leaves.

With further work, label frequencies among all the leaf nodes could be derived from Proposition 11.1 as a function of the color change parameters (ρ_d) and height probabilities (q_s) . It may be possible to move beyond the crude models (2) for color change parameter, and (35) for random height, to fit a color frequency distribution to leaf nodes.

FIGURE 6. **Label frequencies among hidden ancestor graph vertices**

A hidden ancestor graph with 477,290 vertices was generated at 1.6% scale, from parameters in Table 1. Over two hundred distinct labels were generated, and the logs of their frequencies are shown on the vertical axis. Labels are ordered in decreasing order of frequency. The latent tree had depth four, and $\rho_1 = 1$, $\rho_4 = 0$. The demarcation between labels created at depths 1, 2, and 3 is clearly visible.



11.2. Color decomposition of Galton-Watson trees. Consider a Galton-Watson tree (V, T) of depth D with $\text{Poisson}(\mu)$ offspring distribution, rooted at v_o . As explained in Section 2.2, each node at depth $d \in \{1, 2, \dots, D\}$ uses a $\text{Bernoulli}(\rho_d)$ trial to determine whether to start a new color; failure means adopting the parent's color. Here $\rho_1 = 1$. The following color decomposition may be useful in fitting $(\rho_d)_{1 \leq d < D}$ to a desired label frequency distribution.

Proposition 11.1 (COLORED SUBTREES). (a) Let ζ_d denote the number of new colors created at depth d . Then ζ_d has a $\text{Binomial}(m, \rho_d)$ distribution, given $|V_d| = \xi_d = m$.

(b) Suppose color c comes into existence when it is adopted by a node $u \in V$ at level d . Then the set of color c nodes forms a subtree (V_c, T_c) , with depth $D - d$, rooted at u , with $\text{Poisson}(\mu(1 - \rho_{d+k}))$ offspring distribution at depth k below u (i.e. depth $d + k$ below v_o). The random subtrees (T_c) are independent.

(c) Each of the ζ_d colors created at depth $d < D$ has on average

$$(42) \quad \nu_d := \mu^{D-d} \prod_{t=d+1}^D (1 - \rho_t)$$

offspring of the same color among the leaf nodes of (V, T) . In addition ζ_D of the leaves possess newly created colors, each having $\nu_D := 1$ instance.

Proof. Property (a) follows because a $\text{Bernoulli}(\rho_d)$ trial at each of the m nodes at depth d determines whether a new color starts at that node.

As for (b) and (c), suppose node v at depth d has color c . Then a Poisson($\mu(1 - \rho_{d+1})$) number of offspring of v also have color c , and each of these has a Poisson($\mu(1 - \rho_{d+2})$) number of offspring of color c , and so on. This reasoning leads to (42). The independence assertions follows from standard thinning properties of branching processes with Poisson offspring distribution. \square

Remark: As a consistency check between (a) and (c), observe that the expected number of leaves of (V, T) equals the sum over c of the expected number of color c leaves:

$$\sum_{d=1}^D \mu^d \rho_d \left(\mu^{D-d} \prod_{t=d+1}^D (1 - \rho_t) \right) = \mu^D.$$

This holds when $D = 1$ because $\rho_1 = 1$. Continue by induction.

11.3. A one-parameter model of component sizes in the agreement graph. For some large graph we wish to model, a connected components algorithm has been applied to the agreement graph, and the size distribution of these components is available. Each component of the agreement graph is a subset of $\chi^{-1}(a)$, for some $a \in \mathcal{A}$.

We have seen cases in which the top hundred component sizes are well fitted by a Dirichlet process, as follows. Suppose Y_1, Y_2, \dots, Y_m are i.i.d. Beta($1, \delta$) random variables, where the parameter $\delta > 0$ will be fitted in Lemma 11.1. Define

$$X_k := Y_k \prod_{i=1}^{k-1} (1 - Y_i), \quad k = 1, 2, \dots, m,$$

where an empty product is taken to be 1. In the stick-breaking metaphor, X_1 is the left fragment after the first break in $[0, 1]$, X_2 is the left fragment after breaking $[1 - X_1, 1]$, and so on. Take the order statistics of $\{X_1, X_2, \dots, X_m\}$ in decreasing order, i.e.

$$(43) \quad X_{(m)} \geq X_{(m-1)} \cdots \geq X_{(1)}.$$

One way to fit the Dirichlet process model is to compare the sequence (43) to the sequence of proportions of vertices in the m largest components of the agreement graph, taken in decreasing order.

Lemma 11.1 (METHOD OF MOMENTS). *Suppose p is the proportion of vertices which belong to the union of the m largest components of a graph with more than m components. Take*

$$(44) \quad \delta := \frac{1}{(1 - p)^{1/m} - 1}$$

Then the expected sum of the m order statistics (43) is p .

Proof. Each Y_i has mean $1/(1 + \delta)$, and so

$$\mathbf{E}[X_k] = \frac{1}{1 + \delta} \left(\frac{\delta}{1 + \delta} \right)^{k-1}.$$

Sum a geometric series, and simplify, to obtain

$$\sum_{k=1}^m \mathbf{E}[X_k] = 1 - \left(\frac{\delta}{1 + \delta} \right)^m.$$

According to (44), this expression is exactly p . \square

Two topics for future work are: (a) to find conditions on the hidden ancestor graph under which component sizes in the agreement graph match a Dirichlet process model, and (b) predict the parameter δ for a hidden ancestor graph.

Acknowledgments. The author received valuable suggestions from Tim McCollam, Emma Cohen, and Jon Berry; and corrections from Tim Chow, Doug Jungreis, and Kevin Chen.

APPENDIX A. REPEATED WEIGHTED SAMPLING

Random experiment: Suppose $(Y_i)_{i \geq 1}$ are independent, positive real random variables, where Y_i has mean ν_i , variance η_i^2 , and uniformly bounded third moments. Also assume that the (Y_i) satisfy

$$(45) \quad \sup_{n \geq 2} \mathbf{E}[n^2 / (\sum_{\substack{1 \leq j \leq n \\ j \neq i}} Y_j)^2] < \infty, \quad \forall i$$

which holds if the (Y_i) satisfy a Central Limit Theorem.

Fix n , let $S := \sum_1^n Y_i$, and let \mathcal{F}_Y denote the sigma-algebra generated by Y_1, Y_2, \dots, Y_n . Conditional on \mathcal{F}_Y , let Z be a random integer in $\{1, 2, \dots, n\}$, where

$$\mathbf{P}[Z = j \mid \mathcal{F}_Y] = \frac{Y_j}{S}.$$

Let Q be a positive integer random variable, conditionally independent of \mathcal{F}_Y given S , with conditional mean $\alpha S/2$. Let Z_1, \dots, Z_Q and Z'_1, \dots, Z'_Q be independent copies of Z , and let K count **collisions**, i.e. the number of $j \leq Q$ for which $Z_j = Z'_j$:

$$K := \sum_{j=1}^Q \mathbf{1}_{\{Z_j = Z'_j\}}.$$

Lemma A.1 (MEAN COLLISION COUNT). *The unconditional mean of K may be written in terms of*

$$\lambda := \sum_{i=1}^n \nu_i; \quad \Lambda = \sum_{i=1}^n \nu_i^2; \quad \zeta^2 := \sum_{i=1}^n \eta_i^2,$$

as

$$\mathbf{E}[K] = \frac{\alpha}{2} \left(\frac{\zeta^2 + \Lambda}{\lambda} - \frac{2}{\lambda^2} \sum_j \nu_j \eta_j^2 + \frac{\zeta^2 \Lambda}{\lambda^3} + O(n^{-2}) \right).$$

Remark: Suppose $\nu_i = \nu$ and $\eta_i^2 = \eta^2$ for all i . The inner expression becomes

$$(46) \quad \nu + \frac{\eta^2}{\nu} \left(1 - \frac{2}{n} + \frac{1}{n} \right) + O(n^{-2}).$$

Proof. The conditional probability, given \mathcal{F}_Y , of a collision $\{Z_j = Z'_j\}$ is $\sum Y_i^2/S^2$. The mean number of trials, given \mathcal{F}_Y , is $\alpha S/2$. Hence one factor of S cancels, and

$$\mathbf{E}[K \mid \mathcal{F}_Y] = \frac{\alpha}{2} \sum_{i=1}^n \frac{Y_i^2}{Y_1 + \dots + Y_n}.$$

Since expectation and summation commute, it suffices to compute a single summand $\mathbf{E}[g(Y_i, S_i)]$, where

$$S_i := \sum_{j \neq i} Y_j; \quad g(y, s) := \frac{y^2}{y + s}.$$

In this formula, Y_i and S_i are independent, and

$$\mathbf{E}[S_i] = \lambda - \nu_i; \quad \text{Var}[S_i] = \zeta^2 - \eta_i^2; \quad \lambda := \sum_i \nu_i; \quad \zeta^2 = \sum_i \eta_i^2.$$

Let us perform a second order Taylor expansion of $g(y, s)$ around $y = \nu_i$ and $s = \lambda - \nu_i$. First derivatives may be ignored because $\mathbf{E}[Y_i - \nu_i] = 0$, and $\mathbf{E}[S_i - \lambda + \nu_i] = 0$. As for second derivatives, we may also ignore $\partial^2 g / \partial y \partial s$ because $\mathbf{E}[(Y_i - \nu_i)(S_i - \lambda + \nu_i)] = 0$, by independence of Y_i and S_i . Computations show that:

$$(47) \quad \frac{\partial^2 g}{\partial y^2}(y, s) = \frac{2s^2}{(y + s)^3}; \quad \frac{\partial^2 g}{\partial s^2}(y, s) = \frac{2y^2}{(y + s)^3}.$$

As for third derivatives, one may also check:

$$\frac{\partial^3 g}{\partial y^3}(y, s) = -\frac{6s^2}{(y + s)^4}; \quad \max \left(\left| \frac{\partial^3 g}{\partial y^3} \right|, \left| \frac{\partial^3 g}{\partial s^3} \right| \right) \leq \frac{6}{s^2}, \quad \forall y, s > 0.$$

The remainder term in a second order Taylor expansion of the first component around $y = \nu_i$ may be written:

$$R_2(y, s) := g(y, s) - g(\nu_i, s) - (y - \nu_i) \frac{\partial g}{\partial y} - \frac{(y - \nu_i)^2}{2} \frac{\partial^2 g}{\partial y^2},$$

which has the bound:

$$|R_2(y, s)| \leq \frac{|y - \nu_i|^3}{6} \left| \frac{\partial^3 g}{\partial y^3} \right| \leq \frac{|y - \nu_i|^3}{s^2}.$$

By the independence of Y_i and $S - Y_i$, the assumption of finite third moments, and (45),

$$\mathbf{E}[|R_2(Y_i, S - Y_i)|] \leq \mathbf{E}[|Y_i - \nu_i|^3] \cdot \mathbf{E}[(S - Y_i)^{-2}] = O(n^{-2}).$$

Similar arguments apply to other remainder terms in the second order Taylor expansion of $g(y, s)$ around $y = \nu_i$ and $s = \lambda - \nu_i$, some of which have zero mean when y is replaced by Y_i and s by $S_i := S - Y_i$. Thus

$$\mathbf{E}[g(Y_i, S_i)] = g(\nu_i, \lambda - \nu_i) + \frac{1}{2} \frac{\partial^2 g}{\partial y^2} \mathbf{E}[(Y_i - \nu_i)^2] + \frac{1}{2} \frac{\partial^2 g}{\partial s^2} \mathbf{E}[(S_i - \sum_{j \neq i} \nu_j)^2] + O(n^{-2}).$$

After substituting from (47), this simplifies to

$$\frac{\nu_i^2}{\lambda} + \frac{\eta_i^2((\lambda - \nu_i)^2 - \nu_i^2) + \nu_i^2 \zeta^2}{\lambda^3} + O(n^{-2}).$$

Adding over all i , regrouping terms, and multiplying by $\alpha/2$, give the result. \square

Example: Suppose Y_i has mean and variance like that of $\text{log-normal}(\mu, \sigma^2)$, namely

$$\mathbf{E}[Y_i] = c := e^{\mu + \sigma^2/2}; \quad \text{Var}[Y_i] = (e^{\sigma^2} - 1)c^2.$$

After simplification, the formula of Lemma A.1 gives an expected collision count of about

$$c(1 + (e^{\sigma^2} - 1)(1 - 1/n)) = ce^{\sigma^2} + O(n^{-1}) = e^{\mu + 3\sigma^2/2} + O(n^{-1}).$$

APPENDIX B. CONSTRAINED MLE OF LOG-NORMAL PARAMETERS

Suppose $\hat{\mu}$ and $\hat{\sigma}$ are maximum likelihood estimates (MLE) computed as in (38) from a sample (y_i) from a $\text{Normal}(\mu, \sigma^2)$ distribution. Let

$$\varphi := \varphi(y_1, \dots, y_n) := \log \left(\frac{1}{n} \sum_{i=1}^n e^{y_i} \right).$$

Lemma B.1. *The constrained maximum likelihood estimate of $\tau := \sigma^2$, under the linear constraint $\mu = \varphi - \frac{\tau}{2}$, is given in terms of the statistics (38) by*

$$\tau = 2(\sqrt{(\hat{\sigma}^2 + (\varphi - \bar{y})^2 + 1)} - 1).$$

Proof. Abbreviate σ^2 to τ , and substitute $\mu = \varphi - \frac{\tau}{2}$ in the log likelihood for the Normal distribution:

$$\mathcal{L}(\tau) = \log \left((2\pi\tau)^{-n/2} \prod_{i=1}^n \exp(-(y_i - \varphi + \tau/2)^2/2\tau) \right).$$

After subtracting constants, and dividing by $n/2$, the function of τ to be maximized is

$$-\log \tau - \frac{1}{\tau n} \sum_{i=1}^n (y_i - \bar{y} + \bar{y} - \varphi + \tau/2)^2 = -\log \tau - \frac{1}{\tau} (\hat{\sigma}^2 + (\bar{y} - \varphi + \tau/2)^2).$$

The derivative is

$$-\frac{1}{\tau} + \frac{1}{\tau^2} (\hat{\sigma}^2 + (\bar{y} - \varphi + \tau/2)^2) - \frac{(\bar{y} - \varphi + \tau/2)}{\tau}.$$

The zeros of this function on $\{\tau : \tau > 0\}$ are the same as those of

$$(\bar{y} - \varphi + \tau/2)^2 - \tau(1 + \bar{y} - \varphi + \tau/2) + \hat{\sigma}^2.$$

Change variables to $z := \bar{y} - \varphi + \tau/2$, so $\tau = 2(z + \varphi - \bar{y})$. We seek the positive zeros of

$$h(z) := z^2 - 2(z + 1)(z + \varphi - \bar{y}) + \hat{\sigma}^2 = -z^2 - 2z(\varphi - \bar{y} + 1) - 2(\varphi - \bar{y}) + \hat{\sigma}^2.$$

Abbreviate $z_0 := \varphi - \bar{y} + 1$. We are solving the quadratic

$$(z + z_0)^2 = z_0^2 + \hat{\sigma}^2 - 2(\varphi - \bar{y}).$$

If the term on the right is positive, this is:

$$z_1 = \sqrt{(z_0^2 + \hat{\sigma}^2 - 2(\varphi - \bar{y}))} - z_0.$$

Substitute for z_0 , and cancel terms, to obtain

$$z_1 = \sqrt{(\hat{\sigma}^2 + (\varphi - \bar{y})^2 + 1)} - (\varphi - \bar{y} + 1).$$

It is now apparent that the square root is always real. Substitute $\tau = 2(z_1 + \varphi - \bar{y})$ to obtain the result. \square

REFERENCES

- [1] M. Ángeles Serrano and Marián Boguñá. Tuning clustering in random networks with arbitrary degree distributions, *Phys. Rev. E* 72, 036133, 2005
- [2] Aaron Clauset, Cosma Rohilla Shalizi, and M. E. J. Newman. Power-law distributions in empirical data. *SIAM Rev.*, 51(4), 661-703, 2009
- [3] R. W. R. Darling. Sparse random graphs with high mean clustering. In preparation, 2020
- [4] R. W. R. Darling & Mark L. Velednitsky. Anomaly detection and correction in large labeled bipartite graphs, arXiV 1811.04483, 2016
- [5] R. W. R. Darling, David G. Harris, Dev R. Phulara, John A. Proos. The combinatorial data fusion problem in conflicted-supervised learning, arXiv:1809.08723, 2018
- [6] Dimitrios Michail, Joris Kinable, Barak Naveh, John V. Sichi. JGraphT—A Java Library for Graph Data Structures and Algorithms. *ACM Trans. Math. Softw.* 46, 2, Article 16 2020
- [7] Alan Frieze & Michal Karonski. *Introduction to Random Graphs*. Cambridge U. P., 2016
- [8] G. R. Grimmett & D. R. Stirzaker. *Probability and Random Processes*. Oxford U. P., 1992
- [9] Russell Lyons & Yuval Peres. *Probability on Trees and Networks*. Cambridge U. P., 2016
- [10] Michael Mitzenmacher. A brief history of generative models for power law and log-normal distributions. *Internet Mathematics*, Volume 1, 2004
- [11] Daniel Nordman, Alyson Wilson, Cynthia Phillips & Jonathan Berry. Listing triangles in expected linear time on a class of power law graphs. www.researchgate.net, 2010
- [12] Samantha Petti & Santosh Vempala. Approximating sparse graphs: the random overlapping communities model. arXiv:1802.03652, 2018
- [13] J. Pitman. Combinatorial stochastic processes. *Lecture Notes in Mathematics* 1875, 2002
- [14] A. V. Sathanur, S. Choudhury, C. Joslyn, S. Purohit. When labels fall short: property graph simulation via blending of network structure and vertex attributes. *CIKM '17*, 2287-2290, 2017
- [15] C. Seshadri, Tamara G. Kolda, Ali Pinar. Community structure and scale-free collections of Erdős-Rényi graphs. *Physical Review E* 85, 056109, 2012
- [16] Tom A. B. Snijders & Krzysztof Nowicki. Estimation and prediction for stochastic blockmodels for graphs and latent block structure. *J. of Classification* 14:75-100, 1997